RESEARCH PAPER

Fluorescent and mass spectrometric evaluation of the phagocytic internalization of a CD47-peptide modified drug-nanocarrier

Chunlan Liu[1] · Danxia Yu[1] · Fuchun Ge[1] · Limin Yang[1] · Qiuquan Wang[1]

Abstract

$Ru(bpy)_3@SiO_2\text{-}COOH$ and $Ru(bpy)_3@SiO_2@CD47$-peptide nanoparticles (NPs) with fluorescent and mass spectrometric properties were designed and synthesized as the models of drug-nanocarriers. Their phagocytic internalization could be quantitatively measured using more sensitive inductively coupled plasma mass spectrometry (ICPMS) (^{102}Ru) versus traditional laser confocal scanning microscope ($\lambda_{ex/em} = 458/600$ nm) for the first time. Modification of a self-signal trigging CD47-peptide on the NPs' surface decreased internalization by 10 times, $(2.79 \pm 0.21) \times 10^4$ $Ru(bpy)_3@SiO_2\text{-}COOH$ and $(0.28 \pm 0.04) \times 10^4$ $Ru(bpy)_3@SiO_2@CD47$-peptide NPs per RAW264.7 macrophage ($n = 5$). The alkynyl-linked CD47-peptide allowed us to quantify the number (2412 ± 250) of CD47-peptide modified on the NP and the total content (5.14 ± 0.25 amol) of signal regulatory protein α (SIRPα) on the macrophage by measuring the clickable tagged Eu using ICPMS. Furthermore, the interaction between CD47-peptide and SIRPα as well as the changes of the remaining free SIRPα during the internalization process of $Ru(bpy)_3@SiO_2@CD47$-peptide NPs were quantitatively evaluated, providing direct experimental evidence of the longspeculated crucial CD47-SIRPα interaction for drug-nanocarriers to escape internalization by phagocytic cells. Remarkable difference in the internalization ratio of 12.3 ± 4.8 of $Ru(bpy)_3@SiO_2\text{-}COOH$ NPs and 4.3 ± 0.5 $Ru(bpy)_3@SiO_2@CD47$-peptide NPs with and without the protein corona indicated that CD47-peptide still worked when the protein corona formed. Not limited to the evaluation of the NPs studied here, such a fluorescent and mass spectrometric approach is very much expected to apply to the assessment of other drug-nanocarriers designed by chemists and before their medical applications.

Keywords ICPMS · Quantification · Nanodrug · Internalization · CD47-peptide · SIRPα

Introduction

Engineered nanomaterials have been significantly studied in the past two decades, because they were thought to provide a precisely controlled releasing manner for drug delivery. They might display the drugs' biological activity concentrated in the diseased cells and tissues, causing less unwanted adverse events and systemic toxicity, thus being more efficacious and safer [1–3]. However, the delivery efficiencies reported were actually less than 1%, implying that the drugs could not access the diseased cells and tissues at a sufficiently high dose as expected [4]. One of the known reasons is the formation of the so-called protein corona on the surface of a drug-nanocarrier. The protein corona might be associated with the mononuclear phagocyte system (MPS) that consists of the phagocytic cells including monocytes, macrophages and dendritic cells [5–7]. The spontaneously formed protein corona acts as opsonins, directing MPS recognize the drug-nanocarriers as foreign materials and raise their accumulation in liver, spleen and kidney where the phagocytic cells reside [4]. One might be now more aware that this "biological identity" of the nanocarriers is distinct from the "synthetic identity" (the size, shape and surface chemistry) that chemists mainly considered [8]. In order to avoid the internalization by

✉ Qiuquan Wang
qqwang@xmu.edu.cn

[1] Department of Chemistry & the Key Laboratory of Spectrochemical Analysis and Instrumentation, College of Chemistry and Chemical Engineering, Xiamen University, Xiamen 361005, Fujian, China

MPS, which not only decrease the drug delivery efficiency but also cause unwanted toxicity, a myriad of different designs have been attempted so far that exhibited unique physicochemical properties and programmed with a multitude of biological and medical functions. For example, human albumin, agonists of pattern recognition receptors and polyethylene glycol were used as surface modifiers for decreasing influence of the protein corona opsonins while increasing the circulation time [9–13]. In addition, cellular membranes play essential roles in biointerfacing, selfidentification and signal transduction as well as compartmentalization. Macrophage and biomimetic leukocyte even cancer cell membranes were also used to coat the nanocarriers for a long-circulating nanodrug delivery [14, 15].

Cellular membrane glycoprotein CD47 is a "marker-of-self" molecule [16]. CD47's extracellular immunoglobulin (Ig) domain interacts with the extracellular N-terminal Ig V domain of transmembrane protein signal regulatory protein α (SIRPα) on phagocytes. It promotes phosphorylation of tyrosine residues within two typical immunoreceptor tyrosine-based inhibitory motifs (ITIM) located in the SIRPα cytoplasmic tail. The phosphorylated ITIM recruit and activate protein tyrosine phosphatases (PTPase) that have Src homology region 2 (SH2)-domain, SHP-1 and SHP-2. The interaction between SHP-1 and/or SHP-2 and the phosphorylated ITIM of SIRPα disrupts their autoinhibitory activity towards the PTPase domain, triggering enzymatic activity and leading to the dephosphorylation of downstream molecules. This process restricts the phagocytic function by generating the signal of "do not eat me" [17]. As typical paradigms, CD47-expressed erythrocytes can coexist with white blood cells in the blood circulation system [18]; and cancer cells are smart enough to overexpress CD47 for disguising themselves as self-cells to escape from the attack of immune system [19]. Scientists believe that the CD47-modified nanocarriers could also camouflage as self-particles thus inhibit the uptake by the phagocytic cells. For instance, CD47 and its functional peptide were used to modify nanobeads for prolonging the circulation time in nonobese diabetic/severe combined immunodeficient mice. Compared to the control nanobeads, the functional peptide modified nanobeads increased the persistence in the circulation with a mean doubling time of 20 ± 3 min. During which, the methods of gene knockout and antibody blocking were employed to prove that the interaction between CD47 and SIRPα that influenced the internalization process [20]. These biological methods did work in revealing the fact that the decreased internalization degree was related to the CD47-SIRPα interaction. However, such biological methods might induce other not yet understandable cellular changes, developing the similar phenomenon thus leading to an uncertainty and many speculations [21]. In order to directly uncover the interaction between CD47 and SIRPα do suppress the phagocytic internalization process, we proposed a dual fluorescent and mass spectrometric approach (Fig. 1). At first, tris(2,2-
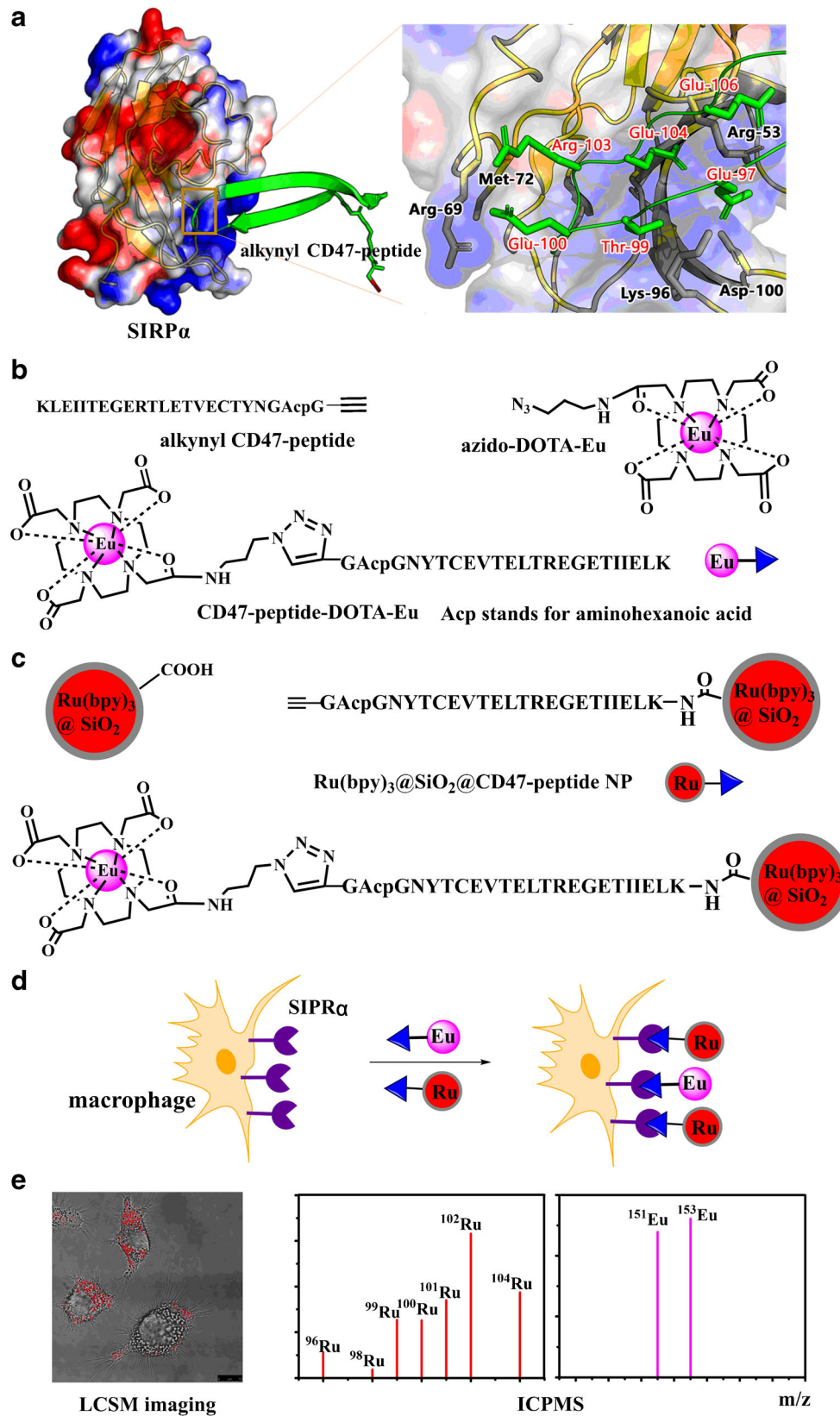
Fig. 1 (**a**) Autodocking of CD47-peptide (green ribbon) in the active site of SIRPα using software autodock 3.0 (http://autodock.scripps.edu), the alkynyl group in the peptide was colored as red. Close-up of the SIRPα active site bound to CD47-peptide was shown in detail at the right hand. The main active amino acid residues (R53, R69, M72, K96, D100) of SIRPα and those (E97, T99, and E100, plus R103, E104, and E106) in CD47 were shown as sticks. (**b**) Amino acid sequence of alkynyl CD47-peptide, and structures of azido-DOTA-Eu and CD47-peptide-DOTA-Eu. (**c**) Ru(bpy)$_3$@SiO$_2$-COOH, Ru(bpy)$_3$@SiO$_2$@CD47-peptide and Ru(bpy)$_3$@SiO$_2$@CD47-peptide-DOTA-Eu. (**d**) Labeling and/or interaction of SIRPα on the macrophages with CD47-peptide-DOTA-Eu and Ru(bpy)$_3$@SiO$_2$@CD47-peptide NPs. (**e**) Visualization and quantification of the internalized NPs using LCSM ($\lambda_{ex/em} = 458/600$ nm) and ICPMS (^{102}Ru), as well as quantification of SIRPα with ^{153}Eu

bipyridyl)dicholororuthenium-(II) (Ru(bpy)$_3$)-doped silica nanoparticles (Ru(bpy)$_3$@SiO$_2$-COOH NPs) was synthesized and used as a model of drug-nanocarriers. Ru(bpy)$_3$@SiO$_2$-COOH NPs was further modified using the alkyne-linked core self-functional amino acids sequence (GAcpGNYTCEVTELTREGETIIELK) of CD47. The obtained Ru(bpy)$_3$@SiO$_2$@CD47-peptide NPs and Ru(bpy)$_3$@SiO$_2$-COOH NPs were used to evaluate the phagocytic internalization process with and without CD47-peptide modification. The internalization process of Ru(bpy)$_3$@SiO$_2$-COOH and Ru(bpy)$_3$@SiO$_2$@CD47-peptide NPs can be visualized and quantified using laser confocal scanning microscope (LCSM) and inductively coupled plasma mass spectrometry (ICPMS), thanks to the fluorescent property of Ru(bpy)$_3$ ($\lambda_{ex/em} = 458/600$ nm) and high sensitive ^{102}Ru signal on ICPMS. Moreover, 1,4,7,10-tetraazacyclododecane-1,4,7-tris-acetic acid-10-(azidopropyl ethylacetamide)-Eu (azido-DOTA-Eu) was used to conjugate alkynyl CD47-peptide via click chemistry for determining the number of CD47-peptide modified on the surface of Ru(bpy)$_3$@SiO$_2$@CD47-peptide NPs. Azido-DOTA-Eu was also click-conjugated directly with CD47-peptide to obtain CD47-peptide-DOTA-Eu for quantifying the total SIRPα on macrophage RAW264.7 and the remained free SIRPα after incubation with the NPs. Influence of the interaction between CD47-peptide and SIRPα on the phagocytic internalization of the NPs can be investigated through measuring ^{153}Eu signals using ICPMS.

Experimental section

Materials and instrumentation

All chemicals used in this study are of at least analytical grade. The ultrapure water used throughout this study was prepared with a Milli-Q system (Millipore Filter Co., Bedford, MA). Triton X-100, tris(2,2-bipyridyl)dicholororuthenium-(II) (Ru(bpy)$_3$), succinic anhydride, 3-aminopropyltriethoxysilane (APTES), tetraethoxysilane (TEOS), 2-morpholinoethanesulfonic acid (MES), 4-morpholinepropanesulfonic acid (MOPS), 1-ethyl-3-(3-dimethylaminopropyl) carbodiimide (EDC) and N-

a

SIRPα

Glu-106
Arg-103 Glu-104 Arg-53
Met-72 Glu-97
Arg-69
Glu-100 Thr-99
Lys-96 Asp-100

alkynyl CD47-peptide

b

KLEIITEGERTLETVECTYNGAcpG—≡

alkynyl CD47-peptide

azido-DOTA-Eu

CD47-peptide-DOTA-Eu

CD47-peptide-DOTA-Eu   Acp stands for aminohexanoic acid

c

Ru(bpy)₃ @ SiO₂ —COOH

≡—GAcpGNYTCEVTELTREGETIIELK—Ru(bpy)₃ @SiO₂

Ru(bpy)₃@SiO₂@CD47-peptide NP

d

SIPRα

macrophage

Eu

Ru

e

LCSM imaging

⁹⁶Ru ⁹⁸Ru ⁹⁹Ru ¹⁰⁰Ru ¹⁰¹Ru ¹⁰²Ru ¹⁰⁴Ru

¹⁵¹Eu ¹⁵³Eu

ICPMS   m/z

hydroxysulfosuccinimide (sulfo-NHS) were purchased from Aladdin Biochemical Polytron Technologies Inc. (Shanghai, China) and used for synthesis of Ru(bpy)₃@SiO₂-COOH NPs. 1,4,7,10-tetraazacyclododecane-1,4,7-tris-acetic acid-

10-(azidopropyl ethylacetamide) (azido-DOTA) was purchased from Macrocyclics (Dallas, TX). Europium oxide (Eu_2O_3, purity ≥99.9%) and sodium ascorbate were obtained from J&K Scientific Ltd. (Beijing, China). Water soluble benzimidazole ligand 5,5′,5′-[2,2′,2″-nitrilotris(methylene)tris(1H-benzimidazole-2,1-diyl)tripentanoic acid tripotassium salt (($BimC4A)_3$) used for copper(I) catalyzed azide-alkyne cycloaddition (CuAAC) reactions was purchased from Sigma-Aldrich (St. Louis, MO). Alkynyl CD47-peptide GAcpGNYTCEVTELTREGETIIELK (CD47-peptide, MW = 2587.7) was designed by us and synthesized by Sangon Biotech (Shanghai) Co., Ltd. (China). Dialysis membranes (molecular weight cut off, 8 kDa) were purchased from Sangon Biotech (Shanghai) Co., Ltd.. Signal regulatory protein α (SIRPα, MW = 64 kDa) was obtained from R&D system (Minneapolis, USA). Bruker Microflex Matrix-assisted laser desorption ionization time of flight mass spectrometry (MALDI-TOF-MS) (Baltimore, MD, USA) was used to determine CD47-peptide and SIRPα adduct. The operational parameters were as follows: cassette N_2 laser, 337 nm; matrix, sinapic acid; and positive ion mode reflectance. For non-radioactive Eu/Ru isotope analysis, an ELAN DRC II ICPMS (PerkinElmer, SCIEX, Canada) equipped with a concentric pneumatic nebulizer and a cyclonic spray chamber. The ICPMS operational parameters were as follows: nebulizer gas, 0.88 L/min; auxiliary gas, 1.0 L/min; plasma gas, 15 L/min; RF power, 1200 W; dwell time, 100 ms; lens voltage, 7.2 V. Parameters such as Ar nebulizer gas flow and lens voltage were optimized daily to obtain the best sensitivity using ELAN DRC II Setup/Stab/Masscal Solution. Transmission electron microscopy (TEM) (JEOL JEM-1400) and dynamic light scattering (DLS) (ZetaSizer Nano ZS, Malvern Instruments) were used for characterization of the NPs. Macrophage cell RAW264.7 and cervical cancer cell HeLa were obtained from the Cell Line Bank of Shanghai Institute for Biological Science. DMEM culture fluid, fetal bovine serum (FBS), penicillin and streptomycin used for cell culture were obtained from ThermoFisher scientific (Waltham, USA). 15-mm-diameter glass bottom cell culture dish and 24-well tissue culture plate were purchased from NEST Biotechnology Co., Ltd. (Wuxi, China). Leica TCS SP5 LCSM (350 to 800 nm) with a HCX PL APL CS 100.0 × 1.40 oil objective and an argon ion laser was used for cell imaging.

Synthesis and characterization of Ru(bpy)$_3$@SiO$_2$-COOH and Ru(bpy)$_3$@SiO$_2$@CD47-peptide NPs

Ru(bpy)$_3$@SiO$_2$-COOH NPs that comprise of Ru(bpy)$_3$ doped silica core and a silica shell were synthesized using a water-in-oil microemulsion system [22]. Briefly, 0.23 mL APTES and 100.0 mg succinic anhydride were first mixed in 0.5 mL DMF to synthesize 3-aminopropyltriethoxysiylsuccinamide. The microemulsion system containing 1.77 mL Triton X-100, 7.5 mL cyclohexane, 1.8 mL n-hexanol, 0.4 mL H_2O and

6.0 mg Ru(bpy)$_3$ was stirred for 1 h, and then 100 μL TEOS and 100 μL ammonium hydroxide were added. After stirred for 24 h, 25 μL TEOS and 70 μL 3-aminopropyltriethoxysiylsuccinamide were added and stirred for another 24 h followed by disturbing the microemulsion medium with acetone and washing with ethanol and water for three times to obtain 40.0 mg Ru(bpy)$_3$@SiO$_2$-COOH NPs. A calibration cure between the concentration of Ru^{3+} (1, 5, 20, 50, 100 ng/mL) and ^{102}Ru signal intensity on ICPMS was made for determination of the average Ru content in one NP. In order to modify CD47-peptide on the surface of Ru(bpy)$_3$@SiO$_2$-COOH NPs through the amidation reaction between amido group in CD47-peptide and carboxyl group on the surface of the NPs, 2.0 mg Ru(bpy)$_3$@SiO$_2$-COOH NPs in 1 mL MES buffer (100 mM, pH 6.0) were mixed with 6.4 mg EDC and 17.6 mg sulfo-NHS and stirred for 15 min to active the carboxyl group, and then the mixture were centrifuged to obtain the precipitate. Subsequently 1 mL MOPS buffer (100 mM, pH 7.5) and CD47-peptide (50 μL, 2 mg/mL) were added and stirred for 2 h to obtain Ru(bpy)$_3$@SiO$_2$@CD47-peptide NPs after five times centrifugation and washing with water. The NPs were all characterized using TEM for morphology. Hydrodynamic diameter (HD) and zeta potential values were detected in MOPS buffer (pH 7.4) and/or 10% FBS medium using DLS.

CD47-peptide content modified on each Ru(bpy)$_3$@SiO$_2$@CD47-peptide NP

To quantify how many CD47-peptide were modified on each Ru(bpy)$_3$@SiO$_2$@CD47-peptide NP, azido-DOTA-Eu tag was used. First, 6.0 mg azido-DOTA was mixed with 4.1 mg Eu(NO$_3$)$_3$ in ammonium acetate buffer (pH 6.4) at 37 °C for 3 h to obtain 6.3 mg azido-DOTA-Eu. Then 1 mg Ru(bpy)$_3$@SiO$_2$@CD47-peptide NPs (corresponding to 1.4 × 10^{12} NPs), in which CD47-peptide was modified with alkynyl group, were mixed with 0.63 mg azido-DOTA-Eu for a 1:1 clickable CuAAC conjugation [23, 24], during which CuSO$_4$ (0.8 mg), (BimC4A)$_3$ (4.5 mg) and sodium ascorbate (9.9 mg) were added and kept 1 h at room temperature. The mixture was then centrifuged, and washed with water for five times to get rid of the excess azido-DOTA-Eu. After HNO$_3$ (7 M, 0.5 mL) was added to the Eu-tagged Ru(bpy)$_3$@SiO$_2$@CD47-peptide NPs and stayed overnight, the nitric acid digested mixture was centrifuged and the supernatant containing Eu was diluted to appropriate concentration for ICPMS analysis (monitoring ^{153}Eu) to know the number of CD47-peptide modified on each Ru(bpy)$_3$@SiO$_2$@CD47-peptide NP.

The internalization of Ru(bpy)$_3$@SiO$_2$-COOH and Ru(bpy)$_3$@SiO$_2$@CD47-peptide NPs by RAW264.7 macrophages

RAW264.7 macrophages were seeded on sterilized 15-mm-diameter glass bottom cell culture dish (1.0 × 10^4 cells per well)

and incubated overnight in DMEM medium containing 10% FBS, 1% penicillin and 1% streptomycin at 37 °C under a 5% CO_2/95% air condition. After washed three times with PBS, 20 μg Ru(bpy)$_3$@SiO$_2$-COOH and Ru(bpy)$_3$@SiO$_2$@CD47-peptide NPs were respectively added to the macrophages and incubated for 0.5, 1.0, 2,0, 5.0, 10.0 and 15.0 h in the culture media with or without FBS. After washing five times with PBS buffer, the cells were first imaged using LCSM, then trypsinized, and centrifuged (2000 r/min, 3 min), the obtained cells were digested with 7 M HNO$_3$ and 10 M HF acids overnight. After gently evaporating out HNO$_3$ and HF acid, the residue was appropriately diluted prior to the determination of Ru in the internalized NPs using ICPMS monitoring ^{102}Ru. Moreover, CD47-peptide was used for block experiments. First, 50 μL 1 mg/mL CD47-peptide was incubated with the macrophages for 3 h and washed five times with PBS, then 20 μg Ru(bpy)$_3$@SiO$_2$-COOH or Ru(bpy)$_3$@SiO$_2$@CD47-peptide NPs were added and incubated for 5 h. In parallel, control experiments were done using SIRPα-negative HeLa cells. 20 μg Ru(bpy)$_3$@SiO$_2$-COOH and Ru(bpy)$_3$@SiO$_2$@CD47-peptide NPs were added respectively to Hela cells and incubated for 24 h, and then washed five times with PBS. All these cells were visualized under LCSM and determined using ICPMS.

SIRPα measurement

Interaction between CD47-peptide and SIRPα was first investigated in vitro. 10 μL 1.0 mg/mL CD47-peptide was added to 20 μL 100 μg/mL SIRPα in 0.5 mL 10 mM PBS buffer (pH 7.4), and the mixture was incubated at 37 °C for 3 h. After the excess free CD47-peptide were dialyzed out, the SIRPα-CD47-peptide adduct was identified using MALDI-TOF-MS with 1 μL sample and sinapic acid (1 μL) as the matrix. Next, a calibration cure between the concentration of SIRPα and the clickable tagged Eu ICPMS intensity was made. CD47-peptide-DOTA-Eu (0.8 mM, 0.1 mL) was added to a series of SIRPα solution (2.4, 12.0, 60.2, 120.0, 150.8 nM) for 3 h each. After dialyzed out of excess CD47-peptide-DOTA-Eu, the SIRPα-CD47-peptide-DOTA-Eu was determined using ICPMS monitoring ^{153}Eu. Finally, SIRPα on RAW264.7 macrophages were quantified. RAW264.7 macrophages (1.0×10^6) were incubated with 20 μg Ru(bpy)$_3$@SiO$_2$-COOH NPs and/or a series concentration (0, 1 ng, 10 ng, 50 ng, 100 ng, 500 ng, 1 μg, 10 μg, 20 μg,

50 μg) of Ru(bpy)$_3$@SiO$_2$@CD47-peptide NPs for 5 h, respectively; afterwards, CD47-peptide-DOTA-Eu (0.8 mM, 0.1 mL) was added. The mixture were further incubated for 5 h. The macrophages were washed five times with PBS, and then 7 M HNO$_3$ digested overnight. After centrifugation and appropriate dilution, the total SIRPα on RAW264.7 macrophage and remained free SIRPα after incubation with the NPs were determined via ICPMS monitoring ^{153}Eu.

Results and discussion

Characterization of Ru(bpy)$_3$@SiO$_2$-COOH and Ru(bpy)$_3$@SiO$_2$@CD47-peptide NPs

From the autodocking of CD47 and SIRPα interaction, we can see that the highest density of CD47 that interacts with the extracellular N-terminal IgV domain of SIRPα is in the loop between canonical β strands F and G containing the amino acids E97, T99 and E100, plus R103, E104, and E106. They are existing in the core self-functional amino acids sequence GNYTCEVTELTREGETIIELK, which locates in the extracellular portion of CD47 [25]. GNYTCEVTELTREGETIIELK peptide was thus modified with alkyne-GAcp to obtain alkynyl CD47-peptide. It was subsequently modified on the surface of Ru(bpy)$_3$@SiO$_2$-COOH NPs via amidation between -COOH and -NH$_2$ at lysine residue of the peptide to obtain Ru(bpy)$_3$@SiO$_2$@CD47-peptide NPs, in which the alkyne was used for later azido-DOTA-Eu labeling through CuAAC click reaction. The synthesized Ru(bpy)$_3$@SiO$_2$-COOH and Ru(bpy)$_3$@SiO$_2$@CD47-peptide NPs were first characterized using TEM and DLS. The obtained TEM results indicated that Ru(bpy)$_3$@SiO$_2$-COOH and Ru(bpy)$_3$@SiO$_2$@CD47-peptide NPs are regularly spherical with uniformly distributed granular diameters of 61.0 ± 3.0 and 63.8 ± 2.0 nm (see Electronic Supplementary Material (ESM) Fig. S1). DLS measurements revealed that the hydrodynamic diameter (HD) of Ru(bpy)$_3$@SiO$_2$-COOH and Ru(bpy)$_3$@SiO$_2$@CD47-peptide NPs were 73.2 ± 0.9 and 77.6 ± 0.3 nm, and negatively charged with the Zeta potentials of -36.5 ± 0.5 and -34.4 ± 0.5 mV ($n = 7$, Table 1). The 4.4 nm and 2.1 mV increases in HD and Zeta potential of Ru(bpy)$_3$@SiO$_2$@CD47-peptide NPs were ascribed to the modification of CD47-peptide, which was about 4 nm and had relative positive potential with an isoelectric point

Table 1 Hydrodynamic diameter (HD) and Zeta potential values of Ru(bpy)$_3$@SiO$_2$-COOH and Ru(bpy)$_3$@SiO$_2$@CD47-peptide NPs in MOPS buffer and FBS medium

Nanoparticle	DLS hydrodynamic diameter (nm)		Zeta potential (mV)	
	MOPS	FBS	MOPS	FBS
Ru(bpy)$_3$@SiO$_2$-COOH	73.2 ± 0.9	110.4 ± 0.9	-36.5 ± 0.5	-25.5 ± 0.9
Ru(bpy)$_3$@SiO$_2$@CD47-peptide	77.6 ± 0.3	110.9 ± 1.8	-34.4 ± 0.5	-25.0 ± 1.1

Septuplicate experiments were performed
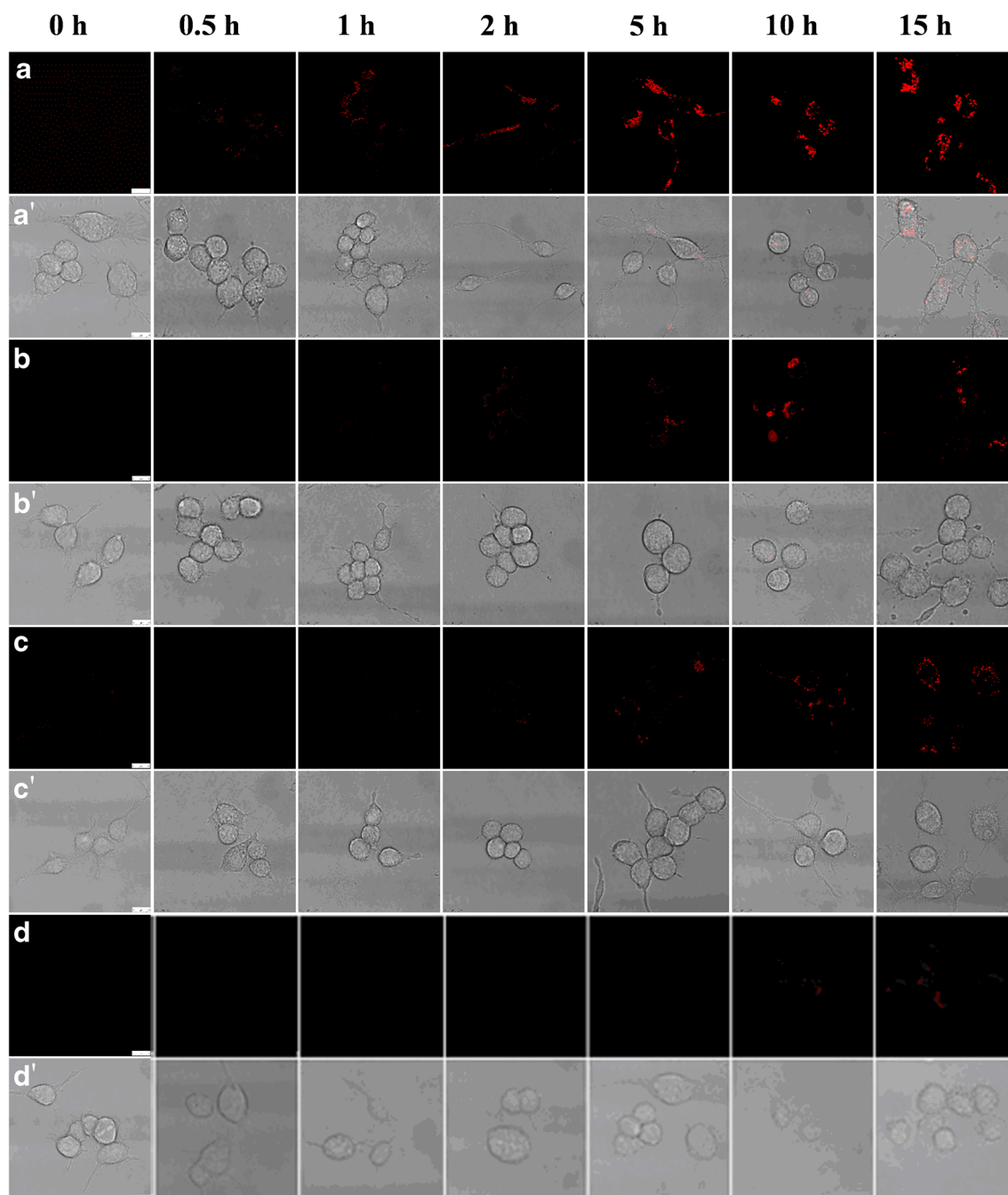
Fig. 2 LCSM images ($\lambda_{ex/em} = 458/600$ nm) of the internalization of Ru(bpy)$_3$@SiO$_2$-COOH and Ru(bpy)$_3$@SiO$_2$@CD47-peptide NPs by RAW264.7 macrophages at different incubation times (0, 0.5, 1, 2, 5, 10, 15 h) with and without FBS. Ru(bpy)$_3$@SiO$_2$-COOH NPs incubated in the culture media with (**a**) and without (**b**) FBS; Ru(bpy)$_3$@SiO$_2$@CD47-peptide NPs incubated in the culture media with (**c**) and without (**d**) FBS, and the corresponding merged fluorescent images (a′, b′, c′ and d′)

of 4 (http://protcalc.sourceforge.net). Subsequently, the average number of CD47-peptide modified on the surface of Ru(bpy)$_3$@SiO$_2$@CD47-peptide NPs was determined using ICPMS by measuring [153]Eu. Based on the 1:1 clickable CuAAC conjugation between azido-DOTA-Eu and alkynyl CD47-peptide, 2412 ± 250 on each Ru(bpy)$_3$@SiO$_2$@CD47-peptide NP were determined. The average Ru content in the NPs was determined by measuring [102]Ru using ICPMS with a known number of the NPs (1.4×10^{12}). The Ru content was 6.4 ± 0.5 zmol (corresponding to 3850 ± 320 Ru atoms) in one Ru(bpy)$_3$@SiO$_2$-COOH and/or Ru(bpy)$_3$@SiO$_2$@CD47-peptide. Moreover, both the NPs emitted red light ($\lambda_{em} = 600$ nm) from Ru(bpy)$_3$ under excitation of $\lambda_{ex} = 458$ nm. As we mentioned before that proteins intend to adsorb on the surface of nanomaterials to form the protein corona when they enter into a biological system. The HDs of both Ru(bpy)$_3$@SiO$_2$-COOH

and Ru(bpy)$_3$@SiO$_2$@CD47-peptide NPs increased to the almost same value of 110.4 ± 0.9 and 110.9 ± 1.8 nm, and also the Zeta potentials to -25.5 ± 0.9 and -25.0 ± 1.1 mV ($n = 7$) after incubated with the culture media containing FBS, indicating that the protein corona was actually formed.

The internalization of Ru(bpy)$_3$@SiO$_2$-COOH and Ru(bpy)$_3$@SiO$_2$@CD47-peptide NPs by RAW264.7 macrophages

RAW264.7 macrophages were used to investigate the phagocytic internalization of Ru(bpy)$_3$@SiO$_2$-COOH and

Ru(bpy)$_3$@SiO$_2$@CD47-peptide NPs. LCSM results showed that Ru(bpy)$_3$@SiO$_2$-COOH NPs (Fig. 2a and a′) could be found clearly inside the macrophages after 0.5 h incubation, but 2 h needed for Ru(bpy)$_3$@SiO$_2$@CD47-peptide NPs (Fig. 2c and c′). While ICPMS results by measuring ^{102}Ru (Fig. 3) indicated that Ru(bpy)$_3$@SiO$_2$-COOH NPs was internalized from 0.5 h incubation as indicated by LCSM, but Ru(bpy)$_3$@SiO$_2$@CD47-peptide NPs were determined after 1 h incubation that is not the same as the observation under LCSM, suggesting that ICPMS not only provide quantitative information but also is more sensitive. After 15 h incubation, the Ru contents in each RAW264.7 macrophage showed

Fig. 3 Calibration curve of Ru concentration against ^{102}Ru signal intensity on ICPMS (a) and average content of Ru in each RAW264.7 macrophage incubated with Ru(bpy)$_3$@SiO$_2$-COOH and Ru(bpy)$_3$@SiO$_2$@CD47-peptide NPs in the culture media with and without FBS for 0.5, 1, 2, 5, 10, 15 h (b). The break for Y axis was from 0.6 to 1 at 60% of the axis
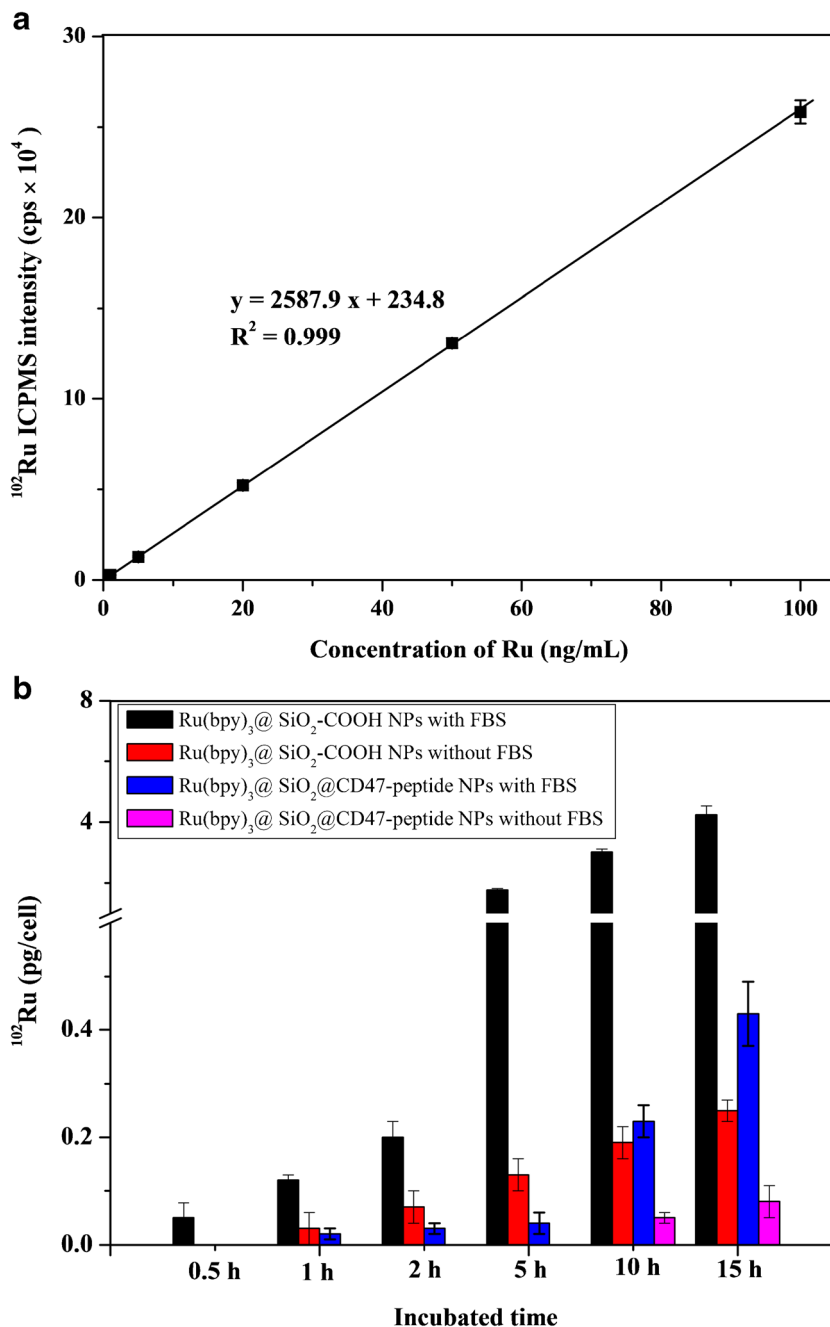
remarkably difference (Fig. 3), 4.24 ± 0.31 pg (corresponding to $(2.79 \pm 0.21) \times 10^4$ NPs) for Ru(bpy)$_3$@SiO$_2$-COOH and 0.43 ± 0.06 pg (corresponding to $(0.28 \pm 0.04) \times 10^4$ NPs) Ru(bpy)$_3$@SiO$_2$@CD47-peptide ($n = 5$). In addition, block experiments using free CD47-peptide were performed to preliminarily verify the influence of CD47-peptide on the internalization. The uptake of both Ru(bpy)$_3$@SiO$_2$-COOH and Ru(bpy)$_3$@SiO$_2$@CD47-peptide NPs by the macrophages became almost negligible when the free CD47-peptide was added 3 h prior to the 5 h incubation with the NPs (see ESM, Fig. S2a$_3$ and a$_4$, and Fig. S3), implying the crucial function of CD47-peptide for escaping the internalization. More importantly, their uptake remarkably decreased when the NPs were incubated with RAW264.7 macrophages in the culture media without FBS, that is, the protein corona was not formed on the surface of the NPs. Especially, Ru(bpy)$_3$@SiO$_2$@CD47-peptide NPs were not internalized until at least 5 h (Fig. 2b, b', d, d', and Fig. 3), suggesting that the protein corona played a very important role in mediating the uptake of the NPs. The internalization ratio of Ru(bpy)$_3$@SiO$_2$-COOH NPs with and without FBS was 12.3 ± 4.8, while that of Ru(bpy)$_3$@SiO$_2$@CD47-peptide 4.3 ± 0.5 after 15 h incubation, indicating that CD47-peptide still worked when the protein corona formed, considering that both Ru(bpy)$_3$@SiO$_2$-COOH and Ru(bpy)$_3$@SiO$_2$@CD47-peptide NPs had the almost same size and Zeta potential after incubated in the culture media containing FBS (Table 1). On the other hand, SIRPα-negative cervical cancer cell Hela was

Fig. 4 MALDI-TOF-MS of SIRPα and the adduct formed by SIRPα and CD47-peptide (**a**) and the calibration curve of SIRPα against ICPMS ^{153}Eu signal intensity (**b**)
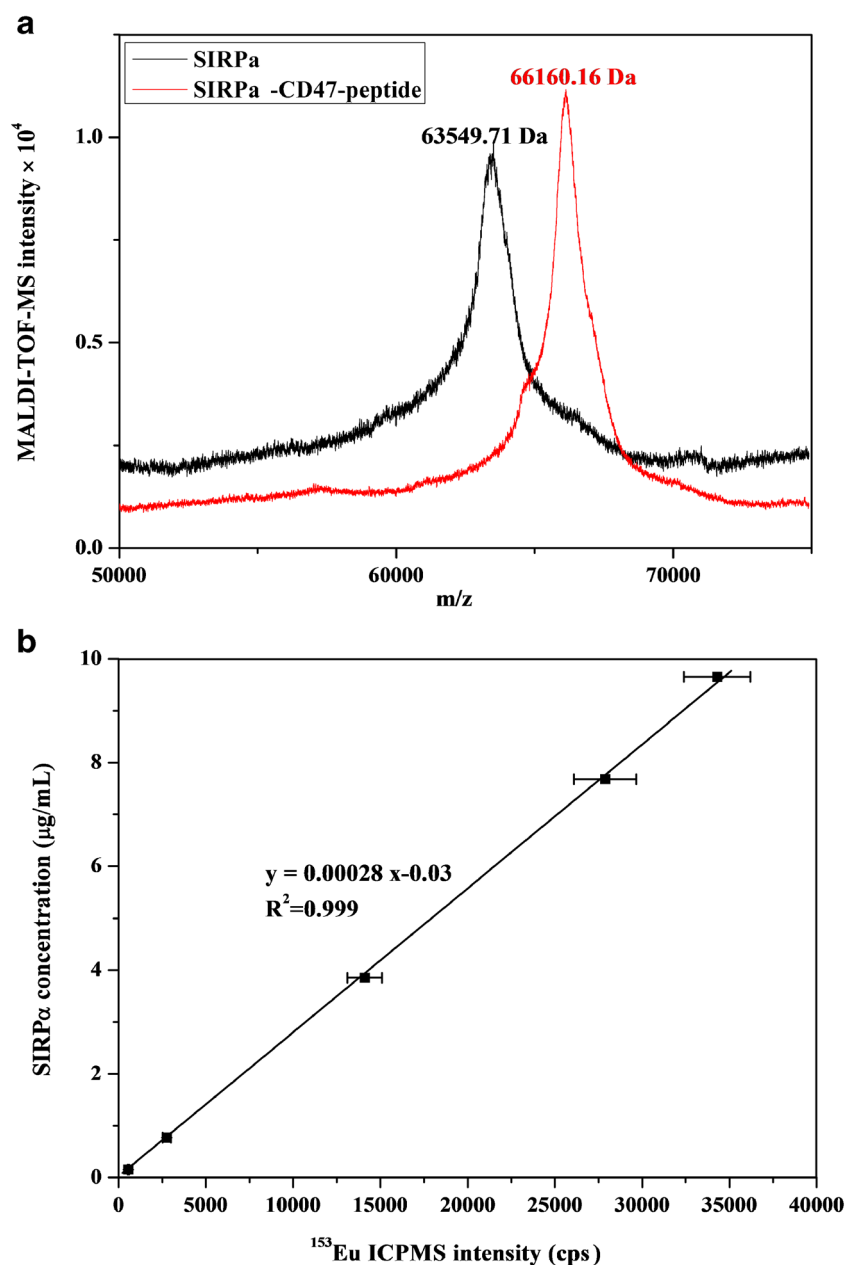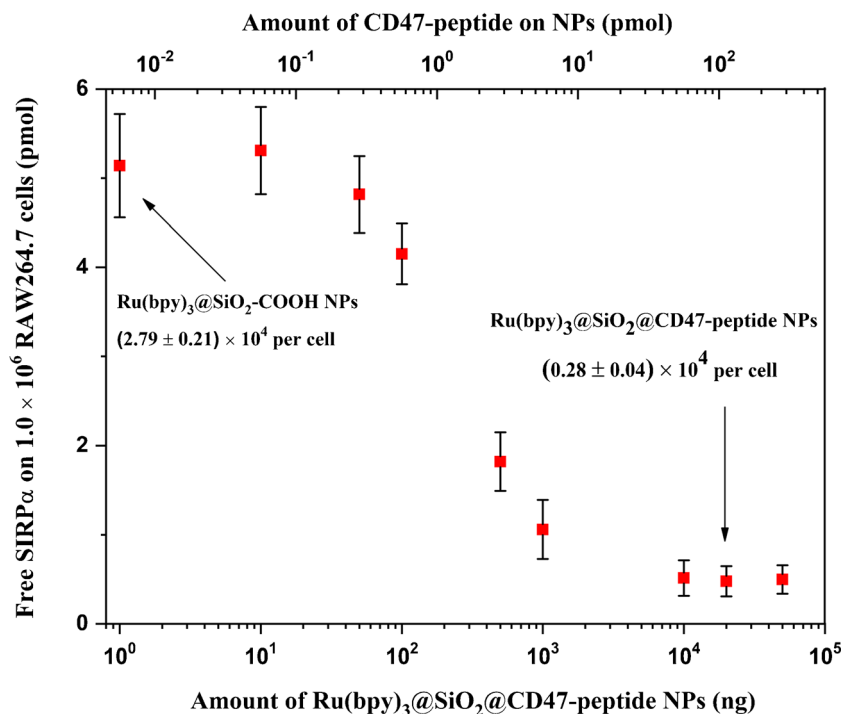
Fig. 5 Free SIRPα content changes on RAW264.7 macrophages when incubated with a series concentration (1 ng, 10 ng, 50 ng, 100 ng, 500 ng, 1 µg, 10 µg, 20 µg and 50 µg) of Ru(bpy)$_3$@SiO$_2$@CD47-peptide NPs. 1.0×10^6 RAW264.7 macrophages were used and five parallel runs were performed

used as a control. The obtained results (see ESM, Fig. S2a$_5$ and a$_6$, and Fig. S3) showed that there were no obvious difference in the uptake by Hela cells between Ru(bpy)$_3$@SiO$_2$-COOH and Ru(bpy)$_3$@SiO$_2$@CD47-peptide NPs, further indicating the indispensable role of the CD47-SIRPα interaction. All these results suggested that the interaction between CD47-peptide and SIRPα is very crucial during the phagocytic internalization process.

Quantitatively evaluation of CD47-peptide and SIRPα interaction

In order to quantitatively evaluate the interaction between CD47-peptide and SIRPα, we first studied the interaction between CD47-peptide (MW = 2587.7 Da) and SIRPα (63,549.71 Da) using MALDI-TOF-MS. As we can see from Fig. 4a, a new peak appeared at 66160.16 Da. The mass difference of 2610.45 ± 25.4 Da ($n = 3$) indicated that one CD47-peptide bound with one SIRPα, which is well in agreement with the autodocking predicated results. Furthermore, we used CD47-peptide-DOTA-Eu as an element-tag to label SIRPα and determine the tagged Eu using ICPMS for establishing a calibration curve of SIRPα concentration against ^{153}Eu signal intensity. The linear dynamic range was up to 150.8 nM (higher concentrations were not tested) with $R^2 = 0.999$ and the LODs (3σ) of 41.1 SIRPα fmol with an RSD of 0.2% at 60.2 nM ($n = 5$) (Fig. 4b), suggesting that we are able to quantify SIRPα using ICPMS by measuring ^{153}Eu. Subsequently, we determined the total free SIRPα content on RAW264.7 macrophages and the remained free SIRPα content after the NPs incubation. The average free SIRPα content on each RAW264.7

macrophage was determined as 5.14 ± 0.25 amol (n = 5) using 1.0×10^6 RAW264.7 cells; the same amount of SIRPα was also determined after the macrophages was incubated for 5 h with 20 µg Ru(bpy)$_3$@SiO$_2$-COOH NPs, owing to no CD47-peptide modified on Ru(bpy)$_3$@SiO$_2$-COOH NPs and thus no interaction with SIRPα. While the remained free SIRPα content more than 10 times decreased to 0.48 ± 0.01 amol (n = 5) after incubated with 20 µg Ru(bpy)$_3$@SiO$_2$@CD47-peptide NPs. Additionally, the remained free SIRPα decreased along with the increase in the amount of not only Ru(bpy)$_3$@SiO$_2$@CD47-peptide NPs added but also CD47-peptide modified on the NPs (Fig. 5), providing the quantitatively experimental evidence of the interaction between CD47-peptide modified on the NPs and SIRPα on the macrophages for the first time.

Conclusions

We designed and synthesized Ru(bpy)$_3$@SiO$_2$-COOH and Ru(bpy)$_3$@SiO$_2$@CD47-peptide NPs as the models of drug-nanocarriers. Their fluorescent and mass spectrometric reporting properties allowed us to investigate the internalization process of the drug-nanocarriers by RAW264.7 macrophages. Modification of the self-signal CD47-peptide on the surface of Ru(bpy)$_3$@SiO$_2$@CD47-peptide NPs significantly decreased its uptake and postponed the starting time of sequestration by RAW264.7 macrophages, implying that Ru(bpy)$_3$@SiO$_2$@CD47-peptide NPs would be less internalized by MPS and have a longer circulation time. The interactions between CD47-peptide and SIRPα during the

internalization process could be quantitatively evaluated using ICPMS with azido-DOTA-Eu tag, providing direct experimental evidence to the long time speculation of CD47-SIRPα interaction, which plays the crucial role for escaping the phagocytic internalization of drug-nanocarriers. Moreover, even though the protein corona formation remarkably induced the NPs internalization, the CD47-peptide modified on the surface of the NPs was still efficacious against the macrophages' uptake. This finding inspire us to modify more effective signal peptides on other drug-nanocarriers for more efficient drug delivery to realize the initial dream of the medical scientists in the near future.

Compliance with ethical standards

Conflict of interest   The authors declare that they have no competing interests.

References

1. Davis ME, Chen ZG, Shin DM. Nanoparticle therapeutics: an emerging treatment modality for cancer. Nat Rev Drug Discov. 2008;7:771–82.

2. Petros RA, DeSimone JM. Strategies in the design of nanoparticles for therapeutic applications. Nat Rev Drug Discov. 2010;9:615–27.

3. Wong PT, Choi SK. Mechanisms of drug release in nanotherapeutic delivery systems. Chem Rev. 2015;115:3388–432.

4. Wilhelm S, Tavares AJ, Dai Q, Ohta S, Audet J, Dvorak HF, et al. Analysis of nanoparticle delivery to tumours. Nat Rev Mater. 2016;1:16014–25.

5. Tenzer S, Docter D, Kuharev J, Musyanovych A, Fetz V, Hecht R, et al. Rapid formation of plasma protein corona critically affects nanoparticle pathophysiology. Nat Nanotechnol. 2013;8:772–81.

6. Cedervall T, Lynch I, Lindman S, Berggård T, Thulin E, Nilsson H, et al. Understanding the nanoparticle-protein corona using methods to quantify exchange rates and affinities of proteins for nanoparticles. Proc Natl Acad Sci U S A. 2007;104:2050–5.

7. Geissmann F, Manz MG, Jung S, Sieweke MH, Merad M, Ley K. Development of monocytes, macrophages, and dendritic cells. Science. 2010;327:656–61.

8. Walkey CD, Chan WCW. Understanding and controlling the interaction of nanomaterials with proteins in a physiological environment. Chem Soc Rev. 2012;41:2780–99.

9. Santos SN, Reis SRR, Pires LP, Helal-Neto E, Sancenón F, Barja-Fidalgo TC, et al. Avoiding the mononuclear phagocyte system using human albumin for mesoporous silica nanoparticle system. Microporous Mesoporous Mater. 2017;251:181–9.

10. Patel PC, Giljohann DA, Daniel WL, Zheng D, Prigodich AE, Mirkin CA. Scavenger receptors mediate cellular uptake of polyvalent oligonucleotide-functionalized gold nanoparticles. Bioconjug Chem. 2010;21:2250–6.

11. Walkey CD, Olsen JB, Guo H, Emili A. Nanoparticle size and surface chemistry determine serum protein adsorption and macrophage uptake. J Am Chem Soc. 2012;134:2139–47.

12. Howard JC, Florentinus-Mefailoski A, Bowden P, Trimbleb W, Grinstein S, Marshall JG. OxLDL receptor chromatography from live human U937 cells identifies SYK(L) that regulates phagocytosis of oxLDL. Anal Biochem. 2016;513:7–20.

13. Vance DT, Dufresne J, Florentinus-Mefailoski A, Tucholskaa M, Trimble W, Grinstein S, et al. A phagocytosis assay for oxidized low-density lipoprotein versus immunoglobulin G-coated microbeads in human U937 macrophages. Anal Biochem. 2016;500:24–34.

14. Fang RH, Jiang Y, Fang JC, Zhang LF. Cell membrane-derived nanomaterials for biomedical applications. Biomaterials. 2017;128:69–83.

15. Blanco E, Shen HF, Ferrari M. Principles of nanoparticle design for overcoming biological barriers to drug delivery. Nat Biotechnol. 2015;33:941–51.

16. Barclay AN, van den Berg TK. The interaction between signal regulatory protein alpha (SIRPα) and CD47: structure, function, and therapeutic target. Annu Rev Immunol. 2014;32:25–50.

17. Matozaki T, Murata Y, Okazawa H, Ohnishi H. Functions and molecular mechanisms of the CD47-SIRPa signalling pathway. Trends Cell Biol. 2009;19:72–80.

18. Oldenborg PA, Zhelenznyak A, Fang YF, Lagenaur CF, Gresham HD, Lindberg FP. Role of CD47 as a marker of self on red blood cells. Science. 2000;288:2051–4.

19. Willingham SB, Volkmer JP, Gentles AJ, Sahoo D, Dalerba P, Mitra SS, et al. The CD47-signal regulatory protein alpha (SIRPα) interaction is a therapeutic target for human solid tumors. Proc Natl Acad Sci U S A. 2012;109:6662–7.

20. Rodriguez PL, Harada T, Christian DA, Pantano DA, Tsai RK, Discher DE. Minimal "self" peptides that inhibit phagocytic clearance and enhance delivery of nanoparticles. Science. 2013;339: 971–5.

21. Rossi A, Kontarakis Z, Gerri C, Nolte H, Hölper S, Krüger M, et al. Genetic compensation induced by deleterious mutations but not gene knockdowns. Nature. 2015;524:230–3.

22. Bagwe RP, Yang CY, Hilliard LR, Tan WH. Optimization of dye-doped silica nanoparticles prepared using a reverse microemulsion method. Langmuir. 2004;20:8336–42.

23. Kolb HC, Finn MG, Sharpless KB. Click chemistry: diverse chemical function from a few good reactions. Angew Chem Int Ed. 2001;40:2004–21.

24. Yan XW, Luo YC, Zhang ZB, Li ZX, Luo Q, Yang LM, et al. Europium-labeled activity-based probe through click chemistry: absolute serine protease quantification using ^{153}Eu isotope dilution ICP/MS. Angew Chem Int Ed. 2012;51:3358–63.

25. Hatherley D, Graham SC, Turner J, Harlos K, Stuart DI, Barclay AN. Paired receptor specificity explained by structures of signal regulatory proteins alone and complexed with CD47. Mol Cell. 2008;31:266–77.

Publisher's note Springer Nature remains neutral with regard to jurisdictional claims in published maps and institutional affiliations.